Innovare
Academic Sciences

International Journal of Pharmacy and Pharmaceutical Sciences

ISSN- 0975-1491 Vol 6, Issue 9, 2014

Original Article

STRUCTURAL OF SUPRAMOLECULAR HYDROGEN BONDING DIOXOURANIUM (VI) COMPLEXES

ASHRAF A. EL-BINDARY*, ABDEL-GHANY F. SHOAIR

Chemistry Department, Faculty of Science, Damietta University, 34517 Damietta, Egypt.
Email: abindary@yahoo.com

Received: 24 Jul 2014 Revised and Accepted: 25 Aug 2014

ABSTRACT

The azodye ligands were synthesized from the coupling of 3-methyl-1-phenyl-1H-pyrazol-5(4H)-one with aniline derivatives and characterized by elemental analyses, IR and NMR spectroscopy. Dioxouranium (VI) complexes of the prepared ligands were characterized by elemental analyses, conductance, thermal analysis and spectral (UV, IR and NMR) results. IR spectra show that the ligands behave as a monobasic bidentate coordinating via the hydrazo nitrogen atom and CO of the pyrazole ring. Thermal studies to verify the status of water molecules inside or outside the coordination sphere of the central metal ion. The optimized bond lengths, bond angles and the calculated quantum chemical parameters for the ligands were investigated. The coordination geometries and electronic structures are determined from a framework for the modeling of the complexes. The force constants, F_{UO} (10^{-8} N/A°) and the bond lengths, R_{UO} (A°) have been calculated from an asymmetric stretching frequency of O-U-O group.

Keywords: Supramolecular structures, Azodye complexes, Dioxouranium (VI), Molecular parameters.

INTRODUCTION

In recent years, UO_2(II) complexes of azodyes ligands have received much attention because of their rich electrochemical and photophysical properties as well as their potential applications in various supramolecular structures as electronics and photomolecular devises [1-5]. Multinuclear systems of this kind can be developed by covalent linking of building blocks with spacers. The size, shape and electronic nature of the bridge controls the electronic communication between the chromophores and thereby the molecule as a whole [6-9].

Azodye ligands play a key role in understanding the coordination chemistry of transition metal ions [5,10]. Hydrogen bonding now is one of the key interactions in the process of molecular aggregation and recognition in nature [6,11,12] and it can be used to design and assemble supramolecular architectures. The development of the field of bioinorganic chemistry has interest in azo dye complexes, since it has been recognized that many of these complexes may serve as models for biologically important species [13,14]. Both the azo dyes and their metal complexes find applications in dye industry. In some cases, the complexes assume more importance due to technical reasons, like better fiber affinity, and light [15] fastness.

El-Sonbati et al. [7,11,12] reported on hydrogen bonded supramolecular quinoline azodyes and/or hydrazono ligands moiety, which can be viewed as hydride structure, composed of a carbonyl/azomethine function and OH/=N-NH group, which has mutual electronic and steric influence on the hydrogen bonding formation dependent on the conformation of the molecules, determined by the two competitive conjugated $\pi - \pi^*$ and $n - \pi^*$ systems and the steric effect. This paper is an extension of previous studies [7,11] in the coordination compounds for several reasons: (i) molecular materials with peculiar electric or optical properties can form intermolecular interactions, required for the desired structural control, differ in nature and they can be provided by, for example, hydrogen bond [12,16] or charge transfer processes [8,10]; (ii) the oxygen bridge with varied stereochemistries has attracted much attention due to their interesting spectral properties and their use in biological processes.

This work deals with synthesis and characterization of azodyes obtained by the coupling of 3-methyl-1-phenyl-1H-pyrazol-5(4H)-one with aniline derivatives and their UO_2(II) complexes. Coordination behavior of the ligands towards UO_2(II) ions was investigated using spectroscopic techniques. The present study, not only aims at the synthesis and characterization of a series of supramolecular metal chelates, but also demonstrates the enhanced effectiveness of charge density on the chelating ring. It also pointed out to the substituents effect on metal ion.

MATERIALS AND METHODS

Materials and physical measurements

The standard chemicals, aniline and its derivatives were purchased from Aldrich chemical company and used as received without further purification. C, H and N were determined on Automatic Analyzer CHNS Vario ELIII, Germany. Spectroscopic data of the ligands and UO_2(II) complexes were obtained using the following instruments: FT-IR spectra (KBr discs, 4000-400 cm^{-1}) by Jasco-4100 spectrophotometer; the ^1H NMR spectrum by Bruker WP 300 MHz using DMSO-d_6 as a solvent containing TMS as the internal standard; the absorbance measurements by UV-visible spectrophotometer (Perkin-Elmer AA800 Model AAS). The uranium content was determined by igniting a definite mass of the complex at 800 °C and weighing the residue as U_3O_8 [17].

Thermogravimetric analysis (TGA) measurements were made using a DuPont 950 thermobalance. Ten milligram samples were heated at 10°/min in a dynamic nitrogen atmosphere (70 ml/min); the sample holder was boat-shaped, 10 × 5 × 2.5 mm deep; the temperature measuring thermocouple was placed within 1 mm of the holder. The molecular structures of the investigated compounds were optimized by HF method with 3-21G basis set.

The molecules were built with the Perkin Elmer ChemBio Draw and optimized using Perkin Elmer ChemBio3D software [18]. El-Sonbati equation [19] has been manipulated by using a computer program developed in our laboratories using C language.

Preparation of 4-(3-derivatives phenylazo)-3-methyl-1-phenylpyrazol-5-one (HL_n)

In a typical preparation [20], 25 ml of distilled water containing 0.01 mol hydrochloric acid were added to *m*-derivatives of aniline (0.01 mole). The resulting mixture was stirred and cooled to 0 ºC. A solution of 0.01 mole sodium nitrite in 20 ml of water was added dropwise.

Formed diazonium chloride was consecutively coupled with an alkaline solution of 0.01 mole 3-methyl-1-phenyl-1H-pyrazol-5(4H)-

one as shown in Scheme 1. The colored precipitate, which formed immediately, was filtered and washed several times with water. The experimental details are given in Scheme 1.

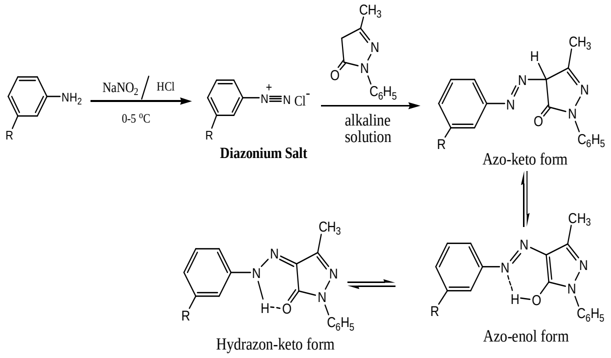

R = -COOH (HL_1); -OH (HL_2) and -OCH_3 (HL_3)

4-(3-carboxyphenylazo)-3-methyl-1-phenylpyrazol-5-one (HL_1).

4-(3-hydroxyphenylazo)-3-methyl-1-phenylpyrazol-5-one (HL_2).

4-(3-methoxyphenylazo)-3-methyl-1-phenylpyrazol-5-one (HL_3).

Scheme 1: Formation mechanism of 4-(3-derivatives phenylazo)-3-methyl-1-phenylpyrazol-5-one.

Preparation of UO_2 (II) complexes

For the synthesis of uranyl complexes; a solution of $UO_2(CH_3COO)_2.2H_2O$ in approximately 50 ml of absolute ethanol was mixed with an appropriate amount of the ligands (HL_n) to give a molar ratio of 1:1 or 1:2. Reflux was continued for 2-3 hrs. The complexes were filtered off and washed with hot ethanol. All precipitates were dried at 40°C. Table 1 shows the details of elemental analysis of the isolated complexes.

RESULTS AND DISCUSSION

Molecular parameters

Based on MO theory [21] the energy terms of the molecular orbital became more closely spaced as the size of the conjugated system increases. Therefore, with every additional conjugated double bond the energy difference between the highest occupied and the lowest vacant π-electron level became smaller and the wavelength of the first absorption band corresponds to this transition is increased. The azo group can act as a proton acceptor in hydrogen bonds [10,22]. The optimized structures of the ligands (HL_n) are given in Fig. 1. The selected geometrical structures of the investigated ligands (HL_n) were calculated by optimizing their bond lengths and bond angles (Tables 2-4). The C(9)-N(8) bond with length 1.273 Å for all ligands (HL_n) is a normal imine bond. From Tables 2-4 the computed net charges on active centers, it is found that the most negative charges in ligands are N(11) & O(24), N(11) & O(17) and N(11) & O(23) for HL_1, HL_2 and HL_3, respectively. Quantum chemical parameters such as the highest occupied molecular orbital energy (E_{HOMO}), the lowest unoccupied molecular orbital energy (E_{LUMO}) and HOMO–LUMO energy gap (ΔE) for the investigated molecules were calculated.

In Fig. 2 the HOMO–LUMO energy gap, ΔE, which is an important stability index, is applied to develop theoretical models for explaining the structure and conformation barriers in many molecular systems [23,24]. The value of ΔE for HL_1, HL_2, and HL_3 was found 0.0655, 0.1024 and 0.1026 a. u., respectively, so ligand (HL_1) more stable and highly reactive than the other ligands (HL_2) and (HL_3) (Table 5). Ligand (HL_1) is more reactive than ligands (HL_2) and (HL_3) as reflected from energy gap values.

The calculated quantum chemical parameters are given in Table 5. Additional parameters such as ΔE, absolute electronegativities, χ, chemical potentials, Pi, absolute hardness, η, absolute softness, σ, global electrophilicity, ω [25], global softness, S, and additional electronic charge, ΔN_{max}, have been calculated according to the following equations [25,26]:

Table 1: Elemental analysis data for the ligands (HL_n) and their UO_2^{2+} complexes[a] (for molecular structures see Scheme 1)[b].

Compound[c]	Code	Exp. (calc.) (%)			
		C	H	N	metal
HL_1		63.55 (63.35)	4.42 (4.35)	17.72 (17.39)	-
$[UO_2L_1(OH_2)(OAc)]2H_2O$	1	32.51 (32.39)	2.72 (2.56)	8.33 (7.96)	34.23 (33.81)
HL_2		65.49 (65.31)	4.85 (4.76)	19.42 (19.05)	-
$[UO_2L_2(OH_2)(OAc)]4H_2O$	2	30.53 (30.34)	2.66 (2.53)	7.24 (8.87)	33.64 (33.43)
HL_3		66.41 (18.23)	5.31 (5.20)	18.38 (66.18)	-
$[UO_2L_3(OH_2)(OAc)]H_2O$	3	34.03 (33.88)	3.34 (3.12)	8.65 (8.32)	35.73 (35.36)
$[UO_2(L_1)_2]H_2O$	4	43.97 (43.87)	2.88 (2.80)	12.23 (12.04)	25.89 (25.59)
$[UO_2(L_2)_2]H_2O$	5	43.44 (43.39)	3.06 (2.98)	13.42 (13.82)	27.54 (27.23)
$[UO_2(L_3)_2]2H_2O$	6	45.41 (45.23)	3.45 (3.33)	12.65 (12.42)	26.54 (26.39)

[a] Microanalytical data as well as metal are in good agreement with the stoichiometry of the proposed , complexes., [b] The excellent agreement between calculated and experimental data supports the assignment in the present work.,[c] HL_1-HL_3 are the ligand as given in Scheme 1 and L_1-L_3 are anions.

$$\Delta E = E_{LUMO} - E_{HOMO}$$

$$\chi = \frac{-(E_{\text{HOMO}} + E_{\text{LUMO}})}{2}$$

$$\eta = \frac{E_{\text{LUMO}} - E_{\text{HOMO}}}{2}$$

$$\sigma = \frac{1}{\eta},$$

$$Pi = -\chi$$

$$S = \frac{1}{2\eta},$$

$$\omega = \frac{Pi^{2}}{2\eta}$$

$$\Delta N_{\max} = -\frac{Pi}{\eta}$$

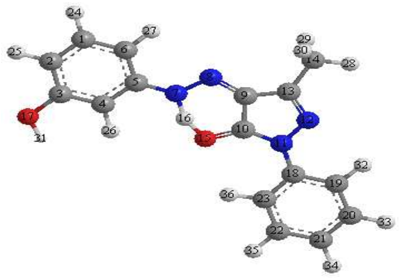

HL₂

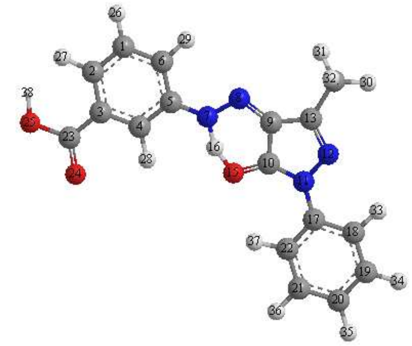

HL₁

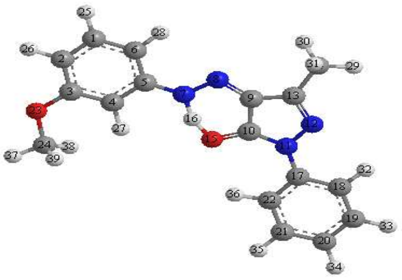

HL₃

Fig. 1: The calculated molecular structures of the investigated compounds (HLₙ).

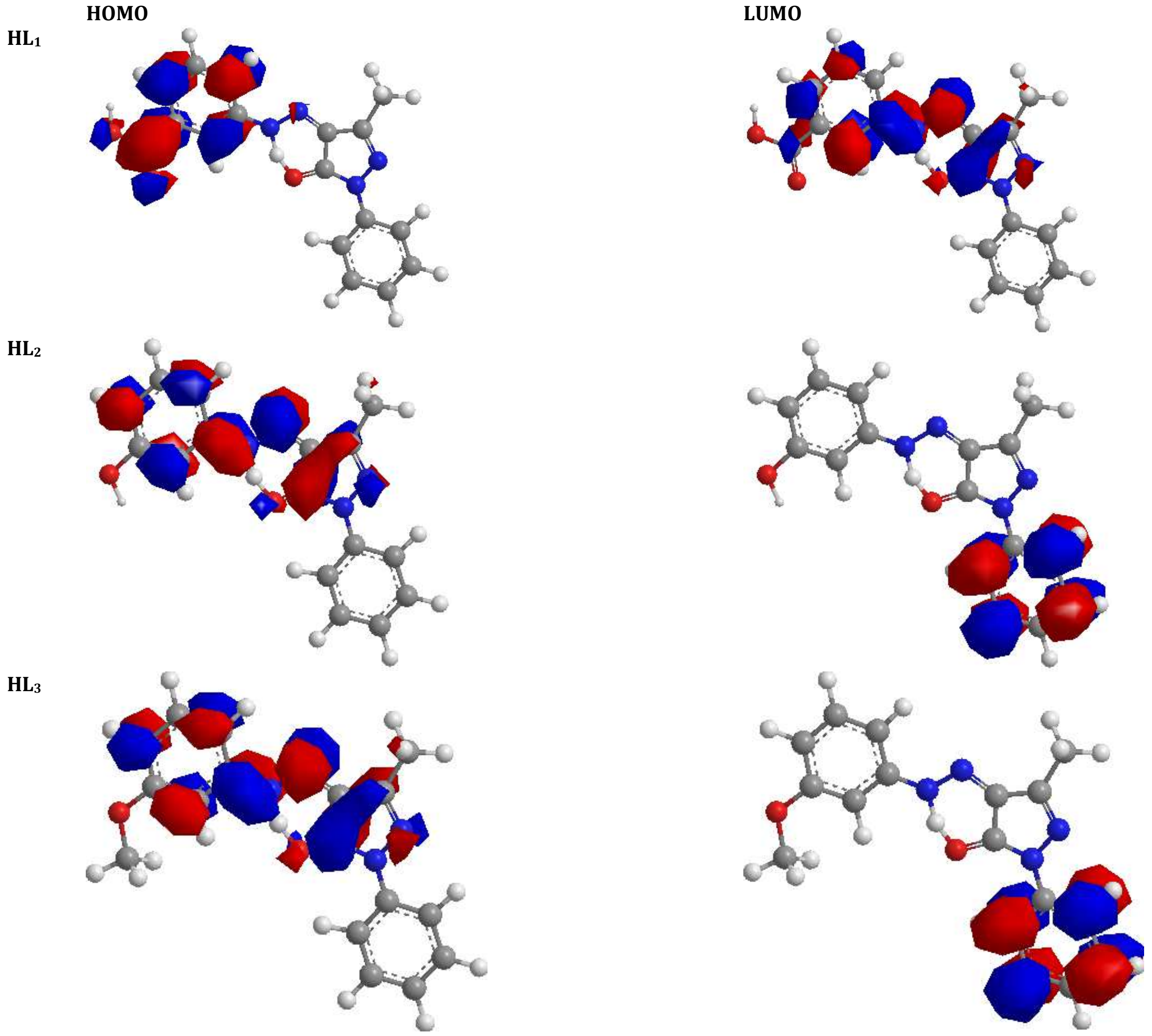

Fig. 2: The Highest Occupied Molecular Orbital (HOMO) and the Lowest Unoccupied Molecular Orbital (LUMO) of the investigated compounds (HLₙ).

Table 2: The selected geometric parameters for HL_1

Bond lengths (Å)		**Bond angles (°)**		**Bond angles (°)**	
O(25)-H(38)	0.968	H(38)-O(25)-C(23)	111.618	H(16)-N(7)-N(8)	108.194
C(22)-H(37)	1.099	H(36)-C(21)-C(22)	120.172	H(16)-N(7)-C(5)	122.63
C(21)-H(36)	1.104	H(36)-C(21)-C(20)	119.498	N(8)-N(7)-C(5)	129.176
C(20)-H(35)	1.102	C(22)-C(21)-C(20)	120.329	H(29)-C(6)-C(1)	117.848
C(19)-H(34)	1.103	H(35)-C(20)-C(21)	120.619	H(29)-C(6)-C(5)	121.572
C(18)-H(33)	1.103	H(35)-C(20)-C(19)	120.618	C(1)-C(6)-C(5)	120.58
C(14)-H(32)	1.114	C(21)-C(20)-C(19)	118.763	C(6)-C(5)-C(4)	118.017
C(14)-H(31)	1.113	H(34)-C(19)-C(20)	119.598	C(6)-C(5)-N(7)	121.087
C(14)-H(30)	1.113	H(34)-C(19)-C(18)	120.209	C(4)-C(5)-N(7)	120.896
C(6)-H(29)	1.103	C(20)-C(19)-C(18)	120.192	C(3)-C(23)-O(25)	121.361
C(4)-H(28)	1.103	H(37)-C(22)-C(17)	122.393	C(3)-C(23)-O(24)	121.637
C(2)-H(27)	1.101	H(37)-C(22)-C(21)	115.188	O(25)-C(23)-O(24)	117.002
C(1)-H(26)	1.104	C(17)-C(22)-C(21)	122.419	H(28)-C(4)-C(5)	117.544
C(1)-C(6)	1.34	H(33)-C(18)-C(19)	115.662	H(28)-C(4)-C(3)	119.997
C(5)-C(6)	1.346	H(33)-C(18)-C(17)	121.817	C(5)-C(4)-C(3)	122.459
C(4)-C(5)	1.349	C(19)-C(18)-C(17)	122.521	C(4)-C(3)-C(2)	117.88
C(3)-C(4)	1.349	C(22)-C(17)-C(18)	115.775	C(4)-C(3)-C(23)	121.649
C(2)-C(3)	1.346	C(22)-C(17)-N(11)	123.712	C(2)-C(3)-C(23)	120.471
C(1)-C(2)	1.341	C(18)-C(17)-N(11)	120.512	H(27)-C(2)-C(3)	122.725
C(17)-C(22)	1.35	H(16)-O(15)-C(10)	109.113	H(27)-C(2)-C(1)	116.606
C(21)-C(22)	1.343	C(17)-N(11)-N(12)	124.253	C(3)-C(2)-C(1)	120.669
C(20)-C(21)	1.339	C(17)-N(11)-C(10)	130.222	H(26)-C(1)-C(6)	119.704
C(19)-C(20)	1.339	N(12)-N(11)-C(10)	105.526	H(26)-C(1)-C(2)	119.901
C(18)-C(19)	1.343	H(32)-C(14)-H(31)	108.417	C(6)-C(1)-C(2)	120.395
C(17)-C(18)	1.352	H(32)-C(14)-H(30)	108.508		
C(3)-C(23)	1.368	H(32)-C(14)-C(13)	109.943		
N(7)-H(16)	1.038	H(31)-C(14)-H(30)	107.938		
O(15)-H(16)	1.006	H(31)-C(14)-C(13)	110.665		
N(11)-C(17)	1.281	H(30)-C(14)-C(13)	111.285		
C(10)-O(15)	1.224	C(13)-N(12)-N(11)	113.35		
C(13)-C(14)	1.495	C(14)-C(13)-C(9)	129.119		
C(13)-C(9)	1.332	C(14)-C(13)-N(12)	123.239		
N(12)-C(13)	1.27	C(9)-C(13)-N(12)	107.633		
N(11)-N(12)	1.25	O(15)-C(10)-N(11)	136.755		
C(10)-N(11)	1.272	O(15)-C(10)-C(9)	111.996		
C(9)-C(10)	1.359	N(11)-C(10)-C(9)	111.248		
N(8)-C(9)	1.273	C(13)-C(9)-C(10)	102.241		
N(7)-N(8)	1.25	C(13)-C(9)-N(8)	136.609		
C(5)-N(7)	1.275	C(10)-C(9)-N(8)	121.15		
C(23)-O(25)	1.36	N(7)-H(16)-O(15)	156.281		
C(23)-O(24)	1.218	C(9)-N(8)-N(7)	113.265		

Negative charge	
N(7)	-0.4271
N(8)	-0.492
C(10)	-0.0238
N(11)	-0.158
N(12)	-0.492
O(24)	-0.57
O(25)	-0.65

Table 3: The selected geometric parameters for HL_2

Bond lengths (Å)		**Bond angles (°)**		**Bond angles (°)**	
C(22)-H(35)	1.103	H(35)-C(22)-C(23)	120.178	H(16)-N(7)-C(5)	122.416
C(20)-H(33)	1.103	H(35)-C(22)-C(21)	119.489	N(8)-N(7)-C(5)	129.271
C(19)-H(32)	1.103	C(23)-C(22)-C(21)	120.334	H(27)-C(6)-C(1)	117.977
O(17)-H(31)	0.971	H(34)-C(21)-C(22)	120.626	H(27)-C(6)-C(5)	121.381
C(14)-H(30)	1.114	H(34)-C(21)-C(20)	120.614	C(1)-C(6)-C(5)	120.642
C(14)-H(29)	1.114	C(22)-C(21)-C(20)	118.76	C(6)-C(5)-C(4)	117.875
C(14)-H(28)	1.113	H(33)-C(20)-C(21)	119.603	C(6)-C(5)-N(7)	121.762
C(6)-H(27)	1.103	H(33)-C(20)-C(19)	120.206	C(4)-C(5)-N(7)	120.364
C(4)-H(26)	1.104	C(21)-C(20)-C(19)	120.192	H(31)-O(17)-C(3)	109.105
C(2)-H(25)	1.103	H(36)-C(23)-C(18)	122.386	H(26)-C(4)-C(5)	120.219
C(1)-H(24)	1.103	H(36)-C(23)-C(22)	115.201	H(26)-C(4)-C(3)	117.174
C(1)-C(6)	1.342	C(18)-C(23)-C(22)	122.413	C(5)-C(4)-C(3)	122.607
C(5)-C(6)	1.346	H(32)-C(19)-C(20)	115.655	C(4)-C(3)-C(2)	117.938
C(4)-C(5)	1.347	H(32)-C(19)-C(18)	121.821	C(4)-C(3)-O(17)	120.738
C(3)-C(4)	1.345	C(20)-C(19)-C(18)	122.524	C(2)-C(3)-O(17)	121.323
C(2)-C(3)	1.343	C(23)-C(18)-C(19)	115.778	H(25)-C(2)-C(3)	119.484
C(1)-C(2)	1.341	C(23)-C(18)-N(11)	123.705	H(25)-C(2)-C(1)	119.698
C(18)-C(23)	1.35	C(19)-C(18)-N(11)	120.518	C(3)-C(2)-C(1)	120.818
C(22)-C(23)	1.343	H(16)-O(15)-C(10)	109.102	H(24)-C(1)-C(6)	120.04
C(21)-C(22)	1.339	C(18)-N(11)-N(12)	124.225	H(24)-C(1)-C(2)	119.839
C(20)-C(21)	1.339	C(18)-N(11)-C(10)	130.258	C(6)-C(1)-C(2)	120.12
C(19)-C(20)	1.343	N(12)-N(11)-C(10)	105.517		

C(18)-C(19)	1.352	H(30)-C(14)-H(29)	108.472	**Negative charge**	
C(3)-O(17)	1.361	H(30)-C(14)-H(28)	108.291	N(7)	-0.4271
N(7)-H(16)	1.038	H(30)-C(14)-C(13)	110.017	N(8)	-0.492
O(15)-H(16)	1.006	H(29)-C(14)-H(28)	108.095	C(10)	-0.0238
N(11)-C(18)	1.281	H(29)-C(14)-C(13)	110.219	N(11)	-0.158
C(10)-O(15)	1.224	H(28)-C(14)-C(13)	111.659	N(12)	-0.492
C(13)-C(14)	1.495	C(13)-N(12)-N(11)	113.367	O(17)	-0.5325
C(13)-C(9)	1.332	C(14)-C(13)-C(9)	128.89		
N(12)-C(13)	1.27	C(14)-C(13)-N(12)	123.485		
N(11)-N(12)	1.25	C(9)-C(13)-N(12)	107.624		
C(10)-N(11)	1.272	O(15)-C(10)-N(11)	136.757		
C(9)-C(10)	1.359	O(15)-C(10)-C(9)	111.996		
N(8)-C(9)	1.273	N(11)-C(10)-C(9)	111.247		
N(7)-N(8)	1.25	C(13)-C(9)-C(10)	102.244		
C(5)-N(7)	1.275	C(13)-C(9)-N(8)	136.557		
		C(10)-C(9)-N(8)	121.199		
		N(7)-H(16)-O(15)	156.233		
		C(9)-N(8)-N(7)	113.159		
		H(16)-N(7)-N(8)	108.312		

Table 4: The selected geometric parameters for HL_3

Bond lengths (Å)		**Bond angles (°)**		**Bond angles (°)**	
C(24)-H(39)	1.113	H(39)-C(24)-H(38)	111.979	C(13)-C(9)-N(8)	136.599
C(24)-H(38)	1.113	H(39)-C(24)-H(37)	108.087	C(10)-C(9)-N(8)	121.168
C(24)-H(37)	1.113	H(39)-C(24)-O(23)	110.392	N(7)-H(16)-O(15)	156.276
C(22)-H(36)	1.099	H(38)-C(24)-H(37)	108.107	C(9)-N(8)-N(7)	113.215
C(21)-H(35)	1.104	H(38)-C(24)-O(23)	110.382	H(16)-N(7)-N(8)	108.241
C(20)-H(34)	1.102	H(37)-C(24)-O(23)	107.745	H(16)-N(7)-C(5)	122.491
C(19)-H(33)	1.103	H(35)-C(21)-C(22)	120.173	N(8)-N(7)-C(5)	129.269
C(18)-H(32)	1.103	H(35)-C(21)-C(20)	119.494	H(28)-C(6)-C(1)	118.102
C(14)-H(31)	1.114	C(22)-C(21)-C(20)	120.333	H(28)-C(6)-C(5)	121.668
C(14)-H(30)	1.113	H(34)-C(20)-C(21)	120.624	C(1)-C(6)-C(5)	120.23
C(14)-H(29)	1.113	H(34)-C(20)-C(19)	120.613	C(6)-C(5)-C(4)	118.124
C(6)-H(28)	1.103	C(21)-C(20)-C(19)	118.763	C(6)-C(5)-N(7)	121.338
C(4)-H(27)	1.102	H(33)-C(19)-C(20)	119.602	C(4)-C(5)-N(7)	120.538
C(2)-H(26)	1.104	H(33)-C(19)-C(18)	120.209	C(3)-O(23)-C(24)	119.007
C(1)-H(25)	1.103	C(20)-C(19)-C(18)	120.189	H(27)-C(4)-C(5)	117.744
C(1)-C(6)	1.34	H(36)-C(22)-C(17)	122.388	H(27)-C(4)-C(3)	118.876
C(5)-C(6)	1.345	H(36)-C(22)-C(21)	115.199	C(5)-C(4)-C(3)	123.381
C(4)-C(5)	1.349	C(17)-C(22)-C(21)	122.413	C(4)-C(3)-C(2)	116.16
C(3)-C(4)	1.349	H(32)-C(18)-C(19)	115.659	C(4)-C(3)-O(23)	125.47
C(2)-C(3)	1.347	H(32)-C(18)-C(17)	121.817	C(2)-C(3)-O(23)	118.37
C(1)-C(2)	1.34	C(19)-C(18)-C(17)	122.525	H(26)-C(2)-C(3)	119.037
C(17)-C(22)	1.35	C(22)-C(17)-C(18)	115.777	H(26)-C(2)-C(1)	118.804
C(21)-C(22)	1.343	C(22)-C(17)-N(11)	123.708	C(3)-C(2)-C(1)	122.159
C(20)-C(21)	1.339	C(18)-C(17)-N(11)	120.515	H(25)-C(1)-C(6)	120.068
C(19)-C(20)	1.339	H(16)-O(15)-C(10)	109.103	H(25)-C(1)-C(2)	119.985
C(18)-C(19)	1.343	C(17)-N(11)-N(12)	124.236	C(6)-C(1)-C(2)	119.946
C(17)-C(18)	1.352	C(17)-N(11)-C(10)	130.256		
C(3)-O(23)	1.375	N(12)-N(11)-C(10)	105.508	**Negative charge**	
N(7)-H(16)	1.038	H(31)-C(14)-H(30)	108.424	N(7)	-0.4271
O(15)-H(16)	1.006	H(31)-C(14)-H(29)	108.498	N(8)	-0.492
N(11)-C(17)	1.281	H(31)-C(14)-C(13)	109.945	C(10)	-0.0238
C(10)-O(15)	1.224	H(30)-C(14)-H(29)	107.943	N(11)	-0.158
C(13)-C(14)	1.495	H(30)-C(14)-C(13)	110.652	N(12)	-0.492
C(13)-C(9)	1.332	H(29)-C(14)-C(13)	111.293	O(23)	-0.3625
N(12)-C(13)	1.27	C(13)-N(12)-N(11)	113.371		
N(11)-N(12)	1.25	C(14)-C(13)-C(9)	129.123		
C(10)-N(11)	1.272	C(14)-C(13)-N(12)	123.241		
C(9)-C(10)	1.359	C(9)-C(13)-N(12)	107.626		
N(8)-C(9)	1.273	O(15)-C(10)-N(11)	136.742		
N(7)-N(8)	1.25	O(15)-C(10)-C(9)	111.997		
C(5)-N(7)	1.275	N(11)-C(10)-C(9)	111.261		
O(23)-C(24)	1.409	C(13)-C(9)-C(10)	102.232		

Structure of the UO_2 (II) complexes

The physical and analytical data of the azodye ligands (HL_n) and their corresponding dioxouranium (VI) complexes are listed in Table 1. Comparing the IR spectra of the complexes with the spectra of the free ligands elucidated the mode of binding of the ligands to the dioxouranium (VI) ions. The complexes have the general formula $[UO_2(L_n)(OH_2)(OAc)]$ and $[UO_2(L_n)_2]$.

The principal ligands (HL_n) undergoes mono deprotonation to form an anion (L_n) in uranyl complexes and acts as a monobasic bidentate ligand coordinating *via* the hydrazo N and CO of pyrazole ring forming two binding chelating sites, thus occupying two positions of an octahedral geometry (Fig. 3).

The acetate and aqua groups occupy the sixth position. All complexes exhibited non-conducting properties in DMF solution.

The formation of the complexes may be represented by the following reactions:

$UO_2(OAc)_2 + HL_n \rightarrow [UO_2L_n(OAc)(OH_2)]$ (1:1, ~ 2h) **(A)**

$UO_2(OAc)_2 + 2HL_n \rightarrow [UO_2(L_n)_2]$ (1:2, ~ 3h) **(B)**

Table 5: The calculated quantum chemical parameters for HL_n

Compound	E_{HOMO} (a. u.)	E_{LUMO} (a. u.)	ΔE (a. u.)	χ (a. u.)	η (a. u.)	σ (a. u.)$^{-1}$	Pi (a. u.)	S (a. u.)$^{-1}$	ω (a. u.)	ΔN_{max}
HL_1	-0.1445	-0.0789	0.0655	0.1117	0.0327	30.525	-0.1117	15.263	0.1904	3.4097
HL_2	-0.08787	0.014516	0.10239	0.0367	0.0512	19.534	-0.0367	9.767	0.0131	0.7164
HL_3	-0.0881	0.0145	0.10261	0.0368	0.0513	19.492	-0.0368	9.746	0.0132	0.7170

(A) **(B)**

Fig. 3: Structures of (A) and (B) products obtained from the reaction of 1:1 and 1:2 molar ratios, respectively.

Infrared spectra

By comparing the IR spectra of the organic ligands (HL_1-HL_3) and their dioxouranium (VI) complexes, the following features can be pointed out:

(1) In the spectra of the ligands (HL_1-HL_3), no characteristic absorption bands assignable to NH_2 function. This confirms the formation of azo compounds.

(2) The strong band observed at 1130–1140 cm^{-1}, which may be assigned to υ(N-N) vibration modes [12,27] is affected on complexation. It is blue shifted and appeared as a weak band.

(3) In all complexes a broad band in the region 3480–3150 cm^{-1} is observed. Such region is attributed to different probabilities: (a) it is due to either free OH or NH; (b) bonded –OH group or –NH group; or (c) due to presence of water molecules.

(4) No characteristic absorption band of the -N=N- function owing to the formation of the hydrazone. The sharp, medium intensity band of C=N (hydrazone) appears at 1595–1575 cm^{-1} for ligands. Additionally, the band due to υ(C=N) (attached to the hydrazo group), was shifted to frequencies lower by 10-30 cm^{-1}, due to chelation with the UO_2(II) ions [28].

(5) The spectra of the ligands exhibit a strong band at ~ 1650 cm^{-1}, which is indicative to υCO. However, the broad band located at 3430 cm^{-1} leads to characterize the υNH rather than hydrogen bonded –OH with -N=N-. This is rather confirmed from the observation of Karabatoses [29] where the hydrazone formed is more than the azo structure for similar compounds.

(6) The band due to υ_{CO} (of the pyrazolone ring) which appeared in the spectra of the ligands were shifted to a higher frequencies by 25-10 cm^{-1} for all complexes. The change in the carbonyl band position [30, 31] in the IR spectra of the metal complexes indicate that the carbonyl group in the hydrazopyrazolone compounds is coordinated to the metals ions (Fig. 3).

(7) The disappearance of the υ(NH) stretching frequency for ligands on chelate formation may be caused by coordination of the hydrazo-nitrogen to the metal ion upon complexation (Fig. 4).

(8) Introduction of a hydrazo group instead of N=N leads to a change in the coordination mode of the azo group from the azo-nitrogen to the amine nitrogen (NH) (Fig. 4).

(9) Coordination of the carbonyl oxygen and the amine nitrogen in the chelate ring is supported by the appearance of new bands which are assigned to U–N and U–O.

(10) The ligand orbitals of hydrazo pyrazolones are group theoretically, energetically and occupationally suitable for participation in both donor (U→L) and acceptor (L→U) π-interactions with the uranyl ion [32]. Convincing evidence [32] has been adduced that U→L π-bonding makes a significant contribution to the bonding in uranyl complexes. This idea is supported by our thermal stability measurements.

(11) The absence of any peak attributed to the -N=N- moiety, implies that the ligands exist predominantly in solution as the form shown in Fig. 4 (1C). However, in solution and in the presence of UO_2(II) ion these compounds exist in a tautomeric equilibrium (1B)↔(1C). The main change is observed in the azo stretching vibration, thus suggesting that the form shown in Fig. 4 (1C) prevails. This tautomeric form losses hydrazono proton when complexed with UO_2 ion as mononegative chelating agents produces the N=N/NH mode of the free ligands. New bands assigned to υ(NH) in the free ligands is absent, suggesting the cleavage of intramolecular hydrogen bonding of υNH group and coordination of nitrogen to the metal ion.

(12) The UO_2(II) complexes exhibits distinct bands at ~ 1635 and 1385 cm^{-1} assignable to υ(C=O) of the coordinated acetate [4,6,22], this is further supported by the appearance of δ(O-C-O) wagging modes of acetate around 680 and 620 cm^{-1} [33]. According to the structure shown in (Fig. 1) the HL_n ligand takes its usual anionic (L_n) to chelate UO_2(II) through N-of hydrazo group and oxygen atom of carbonyl group (Fig. 4) as the potential binding sites, whereas the acetate/aqua anion just fit the remaining free coordination position.

(13) A sharp, intense band ~ 900 cm^{-1} in the spectra of all uranyl complexes is assigned to the asymmetric uranyl stretching frequency υ(U=O) [4,6,7,22].

(14) Bands corresponding to those at 605-615 and 420-460 cm^{-1} in the uranyl complexes were present in nearly all spectra and were the principal bands in the far IR region, exhibiting appreciable substituted sensitivity. Their assignment to υ(U-O) was therefore preferred. Such classes of compounds as illustrated in Scheme 1 have different types of hydrogen bonding (Fig. 4) [3,7,12,34], as follows:

1. Intramolecular H-Bonding of the type O-H···· N between the –OH group and –N=N- group (1B).

2. Intramolecular H-Bonding of the type N–H···· O between the –NH group and C=O group (1C).

3. Intermolecular H-Bonding of the O – H···· N (1D) or N – H···· O (1E). The case (2) is more favored than (1), due to the presence of a broad

band located at 875–975 cm^{-1}, which could be taken as a good evidence for the intermolecular H-Bonding.

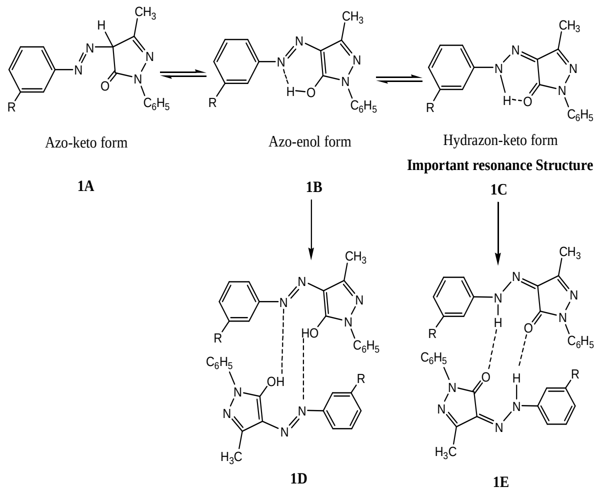

R = -COOH (HL_1); -OH (HL_2); and -OCH_3 (HL_3)

Fig. 4: General formula and proton numbering of the 4-(3-derivatives phenylazo)-3-methyl-1-phenylpyrazol-5-one (HL_n).

^{1}H NMR spectra

The ^{1}H NMR spectra of the ligand (HL_3) and its complex (**3**) have been recorded in DMSO-d_6 using TMS as the internal standard. A broad signal in complex (**3**) observed at 11.20 ppm is attributed to the NH proton and disappear in the presence of D_2O. Further, the CH signal vanishes and a new –C=N and -NH signal appears upon complexation *i. e.* the coordination of nitrogen atom of the hydrazone group with the metal ion [35-37]. This signal disappears upon addition of D_2O *i. e.* change from azo-keto form to hydrazone-keto form.

Electronic spectra

The U. V. spectra of the uranyl complexes exhibit a band in the 20300 – 18800 cm^{-1} region assigned to $^1E^+_g \rightarrow {}^3\pi_u$ transition. This band is similar to the O-U-O symmetric stretching frequency for the first excited state [37]. The bands observed in the spectra of the ligands as well as the uranyl complexes in the 47200 – 47800, 43100 – 43500 and 34400 – 36400 cm^{-1} regions are assigned to Ph – Ph*, π – π* (Phenyl) and n – π* transitions, respectively. Another band at ~34900 cm^{-1} in the spectra of the ligands is assigned to complex formation with UO_2^{2+} [37].

Thermal analysis

Thermal analyses of the UO_2 (II) complexes (1-3) were used to get information about the thermal stability of the complexes as well as to verify the status of water molecules inside or outside the coordination sphere of the central metal ion.

The determined temperature ranges, % losses in mass and thermal effects accompanying the changes in the solid complexes on heating are given in Table 6, which revealed the following findings:

(i) The first decomposition within the temperature range 100-130 ºC may be attributed to the liberation of hydrated molecule.

(ii) The second and third steps are found in the temperature range 130-200 º corresponding to the coordinated water molecules and the coordinated OAc could be eliminated within the range 230-260 ºC [33].

(iii) The fourth step occur within the temperature range 280 – 570 ºC, which may be attributed to the loss of organic part. The remaining mass loss is regarded U_3O_8 as residue.

Stereochemistry and the structure of the uranyl complexes (1-3)

The isolation of HL_n complexes with $UO_2(CH_3COO)_2.2H_2O$ involving 1:1/1:2 UO_2(II):ligand ratio (Table 1) illustrates clearly that the ligands under study does not introduce sufficiently severe steric hindrance as to preclude the formation of $[UO_2(L_n)(OH_2)(OAc)]$ / $[UO_2(Ln)_2]$ complexes, but its steric feature and arrangement in space can also favorable influence the stabilization of complexes.

The IR spectra of all complexes show two bands attributed to the asymmetric and symmetric stretching frequencies. A group theoretical consideration [37] shows that a linear and symmetrical triatomic UO_2(II) ion possessing $\mathbf{D_{\infty h}}$ symmetry gives rise to three fundamental modes of vibrations.

In the equatorial bonding, the more effective overlap of O-U-O group orbital by nitrogen more than oxygen in the ligands leads to lower υ_3 values for UO_2(II) complexes. The force constant of U-O bond in the present investigation has been calculated following McGlynn *et al.*[38], and the U-O bond distance for the corresponding complexes are evaluated using the Jones equation [39,40] where $R_{U-O} = 1.08\ F^{-1/3} + 1.17$. The evaluated values are given in Table 7, and such a report is also found for other uranyl complexes, which is due to the presence of electron donating or electron withdrawing substituents in the equatorial position. El-Sonbati equation [19] has been used to determine the symmetric stretching frequency. The symmetric stretching frequencies are in turn used to evaluate the force constant and bond-bond interaction with neglect of the ligand. The variation of bond length in the complexes is due to presence of electron releasing or electron withdrawing substituents in the equatorial position.

Table 6: Thermogravimetric analysis of some uranyl complexes of ligands (HL_n)

Code*	Complexes	Temp. range (ºC)	Mass loss (%)		Effect type	Assignment
			Calc.	Found		
1	$[UO_2(L_l)(OAc)(OH_2)]2H_2O$	110-120	5.11	4.98	Endo	Loss of two H_2O molecules
		130-170	2.70	2.63	Exo	Loss of one coordinated H_2O molecule
		235-260	9.08	8.88	Exo	Loss of OAc group
		330-340	25.21	24.87	Exo	Loss of organic part (COOH-C_6H_4-N_2)
		350-550	64.71	64.53	Exo	Loss of rest of ligand (phenyl pyrazolon) and formation of metal oxide
2	$[UO_2(L_2)(OAc)(OH_2)]4H_2O$	100-110	10.11	9.78	Endo	Loss of four H_2O molecule
		160-190	2.81	2.75	Endo	Loss of one coordinated H_2O molecule
		260-310	9.49	9.32	Exo	Loss of OAc group
		330-430	21.49	21.33	Exo	Loss of organic part (HO-C_6H_4-N_2)
		450-560	64.71	64.43	Exo	Loss of rest of ligand (phenyl pyrazolon) and formation of metal oxide
3	$[UO_2(L_3)(OAc)(OH_2)]H_2O$	105-130	2.68	2.47	Endo	Loss of one H_2O molecule
		160-198	2.75	2.66	Endo	Loss of one coordinated H_2O molecule
		210-260	9.28	9.17	Exo	Loss of OAc group
		280-470	49.57	49.12	Exo	Decomposition of complex and formation of metal oxide

* See Table 1 and Scheme 1., ^{a} The excellent agreement between calculated and experimental data supports the assignment in the present work

Table 7: Variation force constant (mdyn/A°) U-O bond distances (A°) and frequencies (cm^{-1}) ν_1 and ν_3 of the isolated UO_2^{2+} complexes.

Complex^a	υ_1	υ_3	f_{U-O}	r_1	r_2	$(f^s_{U-O})_t$	r_t	$(f^s_{U-O})_o$	r_o	$(\nu_1^*)^c$	$(f^x_{U-O})_o$	r_3
1	826	900	6.6858	1.743288	1.723928	6.5274	1.747888	6.3629	1.752826	823.95	6.1474	1.759558
2	822	895	6.6117	1.745421	1.727866	6.4615	1.749846	6.3051	1.754601	823.98	6.1111	1.760723
3	817	890	6.5381	1.747573	1.731835	6.3887	1.75204	6.2332	1.75684	824.3	6.0758	1.761865

^{a} The serial number corresponds to that used in the Table 1 and Scheme 1.,^{1,2} Internuclear distance U-O calculated by using Badger equation and Jones equation. ,^{b} $_{U-O}$ Force constant and UO-UO$^-$ interaction constant with neglect the interaction of the UO bonds with the ligands, , ($F_{UO.\ UO^-}$ =bond-bond interactions)., ^{c} Symmetric stretching frequencies evaluated by using El-Sonbati equation., $(F^s_{U-O})_t$ Is the true value of force constant., $(F^s_{U-O})_a$ Is the constant calculated with neglect of the ligands., mF^*_{U-O} Is the bond force constant which evaluated by using El-Sonbati equation., r_t Internuclear distance U-O calculated by using the value of force constant., r_o Internuclear distance U-O calculated by using the asymmetric stretching frequency with neglect of the ligands., r_3 Internuclear distance U-O calculated by using the symmetric stretching frequency evaluated buy using El-Sonbati equation.

Uranyl ion UO_2(II) is quite peculiar both in its own structure and in its coordination compounds [39,40]. The reaction reveals its identity over wide range of vibrations in experimental conditions and can be considered from the geometric point of view, as a single particle. In the present investigation, the υ(U-O) in all the complexes has been shown at 890-900 and 815-830 cm^{-1} regions these bands are assigned to υ_3 and υ_1, respectively (Table 7). The υ_3 values decrease as the donor characteristicly increases as is observed for π-electron substituents, where the basicity of the donating atom increases.

The experimental results reveal an excellent linear relation between υ_1 and υ_3 with the slope corresponding to $(1 + 2\ M_O/M_U)^{1/2}$ (where M_O and M_U are the masses of oxygen and uranium atoms, respectively) (Fig. 5).

The objective in using El-Sonbati equation from which the U-O bond force constant is deduced, should be eventually serve as a fairly accurate measure for the U-O bond distance in given compounds. The force constant for the U-O bond [F_{U-O} 10^{-8} N/A°], $(F^s_{U-O})_t$, and $(F^s_{U-O})_{O^-}$ when neglecting the interaction of the U-O bonds with the ligands and the U-O bond distance [r_{U-O} A°] is determined (Table 7). A plot of $\upsilon_1 + \upsilon_3$ and/or υ_3 versus force constant for the U-O (F_{U-O} 10^{-8} N/A° or F^*_{U-O} 10^{-8}/A°) and the U-O bond distance (r_{U-O} A° or $r_{3\ U-O}$ A°) gives a straight line with an increase in the value of $\upsilon_1 + \upsilon_3$ and/or υ_3 decrease, which accompanied by increase in the force constant of the U-O bond (Figs. 6 and 7). Also, plotting r_1, r_2, r_3 and r_t (bond distance, r_{U-O}) versus υ_3 gives straight lines with increase in the value of υ_3 which accompanied by decrease in r_{U-O} (Fig. 8). The calculation results also showed an inverse relationship between υ_3 and r_{U-O}.

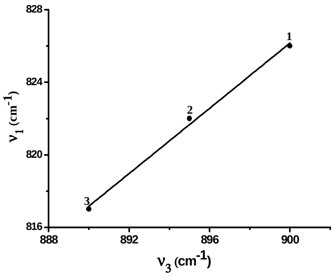

Fig. 5: The relation between ν_1 *vs.* ν_3 (cm^{-1}).

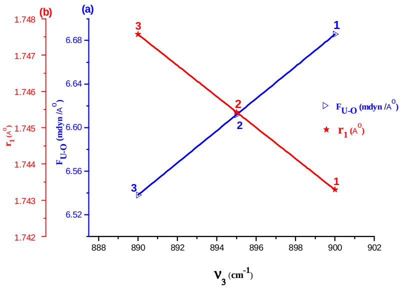

Fig. 6: The relation between ν_3 *vs.* and a) F_{U-O} (10^{-8} N/A°) and b) r_1 (A°).

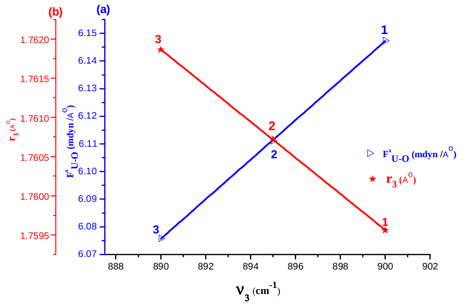

Fig. 7: The relation between r_3 (A°) and F^x_{U-O} (10^{-8} N/A°) with ν_3 (cm^{-1}).

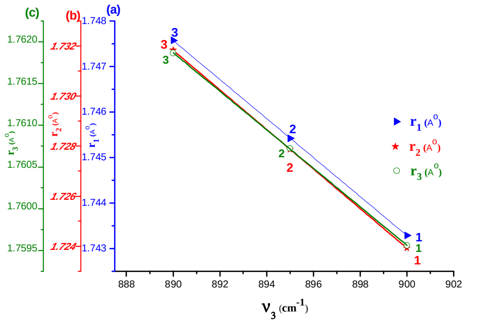

Fig. 8: The relation between ν_3 *vs.* a) r_1, b) r_2 and c) r_3.

CONCLUSION

In this work, the azodye ligands were synthesized from the coupling of 3-methyl-1-phenyl-1H-pyrazol-5(4H)-one with aniline derivatives and characterized by elemental analyses, IR and NMR spectroscopy. Dioxouranium (VI) complexes of the prepared ligands were characterized by elemental analyses, conductance, thermal analysis and spectral (UV, IR and NMR) results. The results of the investigation support the suggested structures of the uranyl complexes and the ligands behave as a monobasic bidentate coordinating via the hydrazo nitrogen atom and CO of the pyrazole ring. The thermal studies verify the status of water molecules inside or outside the coordination sphere of the central metal ion. The optimized bond lengths, bond angles and the calculated quantum chemical parameters for the ligands were investigated. The value of ΔE for HL_1, HL_2 and HL_3 was found 0.0655, 0.1024 and 0.1026 a. u., respectively, so the ligand (HL_1) more stable and highly reactive than the other ligands (HL_2) and (HL_3). The force constants, F_{UO} (10^{-8} N/A°) and the bond lengths, R_{UO} (A°) have been calculated from asymmetric stretching frequency of O-U-O group.

CONFLICT OF INTERESTS

Declared none

REFERENCES

1. Abou-Hussein AA, Linert W. Synthesis, spectroscopic, coordination and biological activities of some organometallic complexes derived from thio-Schiff base ligands, Spectrochim. Acta A 2014;117:763-71.
2. Belser P, Bernhard S, Blum C, Beyeler A, De Cola L, Balzani V. Molecular architecture in the field of photonic devices. Coord Chem Rev 1999;190:155-69.
3. El-Dissouky A, El-Bindary AA, El-Sonbati AZ, Hilali AS. Structural and models of dioxouranium (VI) with rhodanineazodyes. Spectrochim Acta A 2001;57:1163-70.
4. Al-Sarawy AA, El-Bindary AA, El-Sonbati DN. Stereochemistry of new nitrogen containing heterocyclic compound: XII. Polymeric uranyl complexes of hydrazone compounds. Spectrochim Acta A 2005;61:1847-51.
5. El-Dossoki FI, Shoair AF, Hosny NM. Hydroxycoumarineazodye, thermal stability, harmonic vibrational spectra, conductance and pH measurements. J Chem Eng Data 2010;55:267-72.
6. El-Sonbati AZ, El-Dissouky A. Complexing ability of uranyl (VI) with some aroylhydrazone derivatives of 7-carboxaldehyde-8-hydroxyquinoline. Transition Met Chem 1987;12:256-60.
7. Diab MA, El-Bindary AA, El-Sonbati AZ, Salem OL. Supramolecular structure and substituents effect on the spectral studies of oxovanadium (IV) azodyes complexes. J Mol Struct 2012;1018:176-84.
8. Barigellotti F, Flamigni L. Photoactive molecular wires based on metal complexes. Chem Soc Rev 2000;29:1-12.
9. El-Sonbati AZ, Diab MA, El-Bindary AA, Morgan ShM. Coordination chemistry of supramolecular rhodanine azodye sulpha drugs. Inorg Chim Acta 2013;404:175-87.
10. Mubarak AA. Structural model of dioxouranium(VI) with hydrazono ligands. Spectrochim Acta A 2005;61:1163-70.
11. Diab MA, El-Bindary AA, El-Sonbati AZ, Salem OL. Supramolecular structure and substituents effect on the spectral studies of dioxouranium(VI) azodyes complexes. J Mol Struct 2012;1007:11-9.
12. Diab MA, El-Sonbati AZ, El-Bindary AA, Barakat AM. Supramolecular spectral studies on metal-ligand bonding of novel quinolineazodyes. Spectrochim Acta A 2013;116:428-39.
13. Abou-Dobara MI, El-Sonbati AZ, Morgan SM. Influence of substituent effects on spectroscopic properties and antimicrobial activity of 5-(4′-substituted phenylazo)-2-thioxothiazolidinone derivatives. World J Microbiol Biotech 2013;29:119-26.
14. Shoair AF, El-Bindary AA. Synthesis, spectral and catalytic dehydrogenation studies of ruthenium complexes containing NO bidentate ligands. Spectrochim Acta A 2014;131:490-6.
15. Patai SEd. The chemistry of diazonium and diazo groups, John Wiley. Chichester 1978;2.
16. El-Ghamaz NA, El-Mallah HM, El-Sonbati AZ, Diab MA, El-Bindary AA, Barakat AM. Optical properties studies on metal-ligand bonding of novel quinolineazodyes thin films. Solid State Sci 2013;22:56-64.
17. Geffery GH, Bassett J, Mendham J, Deney RC. Vogel's textbook of quantitative chemical analysis, 5th Ed. Longman: London; 1989.
18. El-Ghamaz NA, Ghoneim MM, El-Sonbati AZ, El-Bindary AA, Abd El-Kader MM. Synthesis and optical properties studies of antipyrine derivatives thin films. J Saudi Chem Soc (DOI: 10.1016/j. jscs. 2014.03.010). (Article in Press)
19. El-Sonbati AZ. Stereochemistry of uranyl complexes of new heterocyclic nitrogen containing aldehydes. I. Novel relationship for O-U-O frequencies center. Spectroscopy Lett 1997;30:459-72.
20. Furniss BS, Hannaford AS, Rogers V, Smith PWG, Tatchell AR. Vogels`s text book of practical organic chemistry, 4th Ed. ElBS Longman Group Ltd: London; 1978.
21. Jean Y. Molecular orbitals of transition metal complexes. Oxford: Université Paris-Sud; 2004.
22. El-Sonbati AZ, Diab MA, El-Shehawy MS, Moqbal M. Polymer complexes: XLX. Novel supramolecular coordination modes of structure and bonding in polymeric hydrazonesulpha drugsuranyl complexes. Spectrochim Acta A 2010;75:394-405.
23. El-Ghamaz NA, El-Sonbati AZ, Diab MA, El-Bindary AA, Awad MK, Morgan SM. Dielectrical, conduction mechanism and thermal properties of rhodanineazodyes. Mater Sci Semicond Process 2014;19:150-62.
24. Feng Y, Chen S, Guo W, Zhang Y, Liu G. Inhibition of iron corrosion by 5,10,15,20-tetraphenylporphyrin and 5,10,15,20-tetra-(4-chloro phenyl) porphyrin adlayers in 0.5 M H2SO4 solutions. J Electroanal Chem 2007;602:115-22.
25. Geerlings P, De Proft F, Langenaeker W. Conceptual density functional theory. Chem Rev 2003;103:1793-847.
26. Yousef TA, Abu El-Reash GM, Al-Jahdali M, El-Rakhawy ER. Structural and biological evaluation of some metal complexes of vanillin-4N-(2-pyridyl) thiosemicarbazone. J Mol Struct 2013;1053:15-21.
27. El-Sonbati AZ, Diab MA, Belal AAM, Morgan ShM. Supramolecular structure and spectral studies on mixed-ligand complexes derived from β-diketone with azodyerhodanine derivatives. Spectrochim Acta A 2012;99:353-60.
28. Shoair AF. Catalytic activity of some new copper(II) azo-complexes. J Coord Chem 2012;65:3511-8.
29. Abu-El-Halawa R, Al-Nuri M, Mahmoud F. Synthesis and antimicrobial activity of new N-methyl-N-(2-pyridyl) aromatic and heteroaromatic hydrazine. Asian J Chem 2007;19:1658-66.
30. El-Sonbati AZ, Diab MA, El-Bindary AA, Abou-Dobara MI, Seyam HA. Supramolecular coordination and antimicrobial activities of constructed mixed ligand complexes. Spectrochim Acta A 2013;104:213-21.
31. El-Sonbati AZ, Diab MA, El-Bindary AA, Abd El-Kader MK. Supramolecular and structural modification on conformational by mixed ligand. Spectrochim Acta A 2012;99:211-7.
32. El-Sonbati AZ, Diab MA, El-Bindary AA, Morgan SM. Supramolecular spectroscopic and thermal studies of azodye complexes. Spectrochim Acta A 2014;127:310-28.
33. El-Sonbati AZ, El-Bindary AA, El-Mosalamy EH, El-Santawy EM. Thermodynamics of substituted pyrazolone. VIII. Potentiometric, spectrophotometric, and conductometric studies of 4-(4-nitrophenylazo)-3-methyl-1-(2-hydroxy-3-morpholinopropan-1-yl)-2-pyrazolin-5-one and its metal complexes. Chem Papers 2002;56:299-304.
34. El-Sonbati AZ, Belal AAM, El-Gharib MS, Morgan SM. Supramolecular structure, mixed ligands and substituents effect on the spectral studies of oxovanadium(IV) complexes of bioinorganic and medicinal relevance. Spectrochim Acta A 2012;95:627-36.
35. Mubarak AT, El-Sonbati AZ, Ahmed SM. Supramolecular structural and spectral perspectives of novel ruthenium(III) azodye complexes. J Coord Chem 2007;60:1877-90.
36. El-Sonbati AZ, El-Bindary AA, Shoair AF. Stereochemistry of new nitrogen containing heterocyclic aldehyde. VIII. Spectral and coordination modes of mixed-ligand of novel ruthenium(III) complexes. Spectrochim Acta A 2002;58:3003-9.
37. Yacouta-Nour A, Maki AK, Mostafa MM, Ibrahim KM, El-Bindary AA. Dioxouranium(VI) complexes of aliphatic (mono and di) hydrazine-oximes. Transition Met Chem 1991;16:23-7.
38. McGlynn SP, Smith JK, Neely WC. The electronic structure, spectra, and magnetic properties of actinyl ions: Part I. The uranyl ion. J Chem Phys 1961;35:105-16.
39. Jones LH. Systematics in the vibrational spectra of uranyl complexes. Spectrochim Acta A 1958;10:395-403.
40. Ibrahim KM, Shallaby AM, El-Bindary AA, Mostafa MM. Dioxouranium(VI) complexes of 3-benzamidorhodanine and its substituted derivatives. Polyhedron 1986;5:1105-8.